J Mater Sci (2025) 60:19236–19248

Metals & corrosion

Enhancing post-bonding oxidation resistance of low-pressure Cu sintered joints via residual reductant retention

Tomoki Matsuda[1,*], Shio Okubo[1], Makoto Kambara[1], and Akio Hirose[1]

[1] *Division of Materials and Manufacturing Science, Graduate School of Engineering, The University of Osaka, 2-1 Yamadaoka, Suita, Osaka 565-0871, Japan*

Received: 5 June 2025
Accepted: 9 September 2025
Published online: 26 September 2025

ABSTRACT

Cu sinter bonding using fine particles is a promising technology for advanced semiconductor packaging requiring enhanced thermal reliability. However, oxidation during the bonding and subsequent high-temperature exposure critically degrades joint integrity. Conventional oxidation mitigation methods employing either high bonding pressures or protective atmospheres present practical limitations for applications. This study demonstrates a low-pressure bonding approach utilizing submicron Cu particles mixed with reducing solvent-based pastes to impart oxidation resistance through the intentional retention of residual solvents in the sintered structure. We systematically investigated the effect of bonding atmosphere (either air or nitrogen) on the post-bonding oxidation resistance during prolonged exposure to ambient air at 250 °C. Joints bonded in air rapidly oxidized, forming continuous Cu_2O layers accompanied by severe mechanical degradation and a tenfold increase in electrical resistivity. In contrast, joints bonded under nitrogen exhibited remarkable oxidation resistance due to suppressed solvent combustion, resulting in residual solvent preservation within the sintered matrix. Thermal and microstructural analyses confirmed that these retained solvents actively inhibited oxidation during subsequent high-temperature storage. The preserved metallic Cu network ensured sustained mechanical integrity and electrical conduction. This low-pressure approach effectively leverages residual reducing solvents, demonstrating substantial potential for achieving oxidation-resistant Cu sintered joints suitable for highly reliable next-generation semiconductor packages.

Handling Editor: Nima Haghdadi.

Address correspondence to E-mail: t-matsu@mapse.eng.osaka-u.ac.jp

https://doi.org/10.1007/s10853-025-11525-x

Introduction

Sinter bonding using metallic fine particles has attracted attention in next-generation semiconductor packaging technologies that require high thermal resistance and reliability. As the particle size decreases to the nanoscale, the sinterability is enhanced owing to the increase in specific surface area [1, 2]. Accordingly, sinter bonding processes employing nano to microscale particles—particularly Ag and Cu—have been developed. Cu sintering processes are more desirable for industrial applications due to their lower cost and improved resistance to electrochemical migration compared to Ag [3]. However, its higher chemical affinity for oxygen makes it particularly susceptible to oxidation during bonding and during device operation.

Thus, conventional approaches for Cu sinter bonding have typically relied on increasing bonding pressure to improve densification and limit oxygen diffusion [3–6], or on conducting bonding in reducing or inert gas atmospheres [3, 7–10]. Furthermore, it has been reported that porous Cu-sintered structures exposed to temperatures above 200 °C in air undergo progressive oxidation to form Cu_2O and CuO [11–13], which degrades both electrical and thermal conductivities [14]. Additionally, oxidation-induced outward diffusion of Cu atoms can generate voids within Cu cores [15, 16], leading to deterioration in mechanical properties. Therefore, achieving a Cu-sintered structure with suppressed oxidation under low-pressure bonding conditions is considered essential for the development of high-performance electronic packages.

Recent studies have revealed that interparticle sintering during the Cu sintering process is facilitated by nanoscale bridging between reduced Cu derived from Cu oxides [8, 17–20]. Notably, pressureless bonding has been successfully achieved through the in situ generation of Cu nanoparticles via reduction of thin surface oxide layers on submicron Cu particles [21, 22]. Furthermore, Cu oxides can be effectively reduced not only in reducing gas atmospheres but also via redox reactions with polyol-based organic solvents [17, 20, 23]. Previous reports have indicated that organic solvent residues effectively suppress post-bonding oxidation under high-temperature storage in air [23]. Similarly, introducing organic compounds into bonding pastes or applying organic protective layers has also been reported to delay oxidation [5, 6, 9, 24].

Based on these findings, fabricating oxidation-resistant Cu-sintered joints under low-pressure conditions would be achievable through redox reactions involving organic solvents and mildly oxidized submicron Cu particles. In particular, suppressing combustion of organic solvents during bonding to ensure their residual presence is expected to further delay oxidation during subsequent exposure to high-temperatures in air. Thus, the present study investigates the influence of bonding atmosphere on the oxidation behavior of Cu-sintered joints fabricated from submicron Cu particles and reducing solvent-based pastes during subsequent exposure to air at 250 °C, a condition known to accelerate Cu oxidation.

Experimental procedure

Submicron Cu particles (particle size: 300–500 nm) [21] were used for bonding. Figure 1 shows the field-emission scanning electron microscopy (SEM), high-resolution transmission electron microscopy (TEM) images, and the X-ray diffraction (XRD) pattern of Cu particles, where a slight Cu_2O layer was formed on the surface of raw particles. Submicron Cu particle paste was prepared by mixing Cu particles with polyethylene glycol

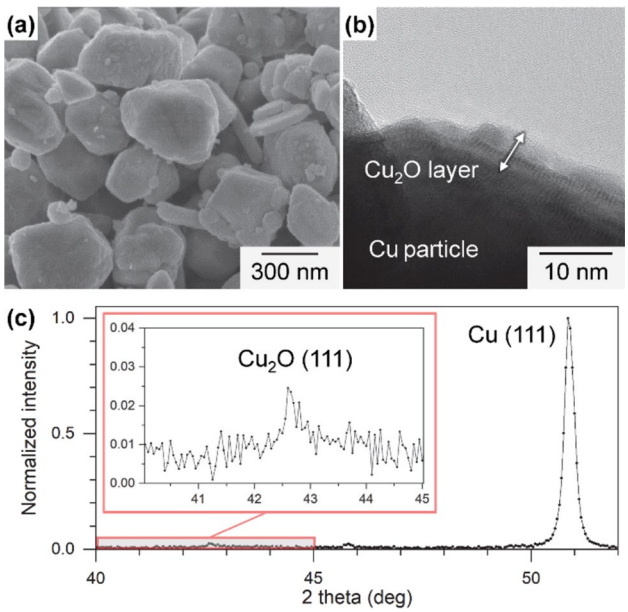

Figure 1 Submicron Cu particles. **a** SEM image. **b** High-resolution TEM image. **c** XRD pattern showing a slight presence of Cu_2O.

400 (PEG400) as a reducing organic solvent and terpineol as a viscosity modifier.

For the sinter bonding experiments, bare Cu disks (5 mmφ × 2 mmt and 10 mmφ × 5 mmt) were used as the bonding specimens. Cu paste with a thickness of 50 μm was screen-printed on the lower Cu disk and preheated to 120 °C for 10 min in air atmosphere to evaporate any excess organic solvent. After the preheating, the sample was heated to the bonding temperature of 300 °C at a rate of 1 °C/s under air or N_2 atmosphere and held for 5–30 min at a bonding pressure of 0.3 MPa. The sintered joint was stored at 250 °C in a high-temperature chamber under air atmosphere to evaluate its thermal durability.

Die-shear strength and resistance measurements of joints were performed before and after the high-temperature storage test. The joint strength was measured by a shear test with a displacement rate of 0.1 mm/s using a bond tester. Figure 2 shows the resistance measurement using the 4-terminal method to measure the resistance between holes. Volume resistivity ρ can be expressed as $\rho = (R - R_{Ref}) \times A/L$, where R is the measured resistance value including the sintered layers, R_{Ref} is the resistance value excluding the sintered layers, A is the cross-sectional area, and L is the total thickness of the sintered layers.

To evaluate the reaction behaviors of the bonding pastes, simultaneous thermogravimetry and differential thermal analysis (TG–DTA) measurements at a heating rate of 1 °C/s were performed. The fractured surface after the shear test and the joint cross-section were observed using stereomicroscopy (SM) and FE-SEM. XRD measurement using the two-theta/theta method was also performed on the bonding materials and fractured surfaces to investigate the oxidation behavior of joints bonded in air and N_2 atmosphere.

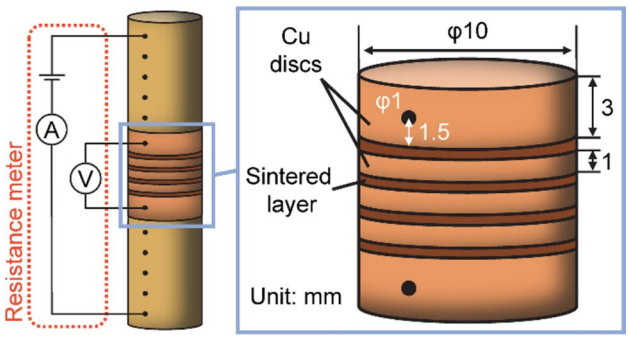

Figure 2 Schematic illustration of the resistance measurement of the sintered layer.

The detailed microstructure of the sintered joint was investigated using TEM and scanning TEM (STEM) observations. The joint cross-section was prepared by Ar-ion milling using a cross-section polisher, and the TEM specimen was fabricated by a focused-ion-beam SEM (FIB-SEM). A composition analysis was performed using energy-dispersive X-ray spectroscopy (EDX) and nanobeam electron diffraction analyses under STEM observation.

Results and discussion

Characteristics of initial joints

Figure 3 shows the strength results of Cu-Cu specimens bonded under low-pressure conditions at 300 °C in both air and N_2 atmospheres. It was observed that bonding in air resulted in higher joint strength compared to bonding in N_2. On the other hand, with increasing holding time during bonding, the joint strength increased in the N_2 atmosphere, whereas a decreasing trend in joint strength was observed for bonding in air.

Figure 4 presents the stereomicroscope observations of the fracture surfaces after shear testing, as well as SEM observations of the copper-sintered regions on the same surfaces. The stereomicroscope results revealed that, for bonding in air, the central part of the joint exhibited a copper-colored fracture,

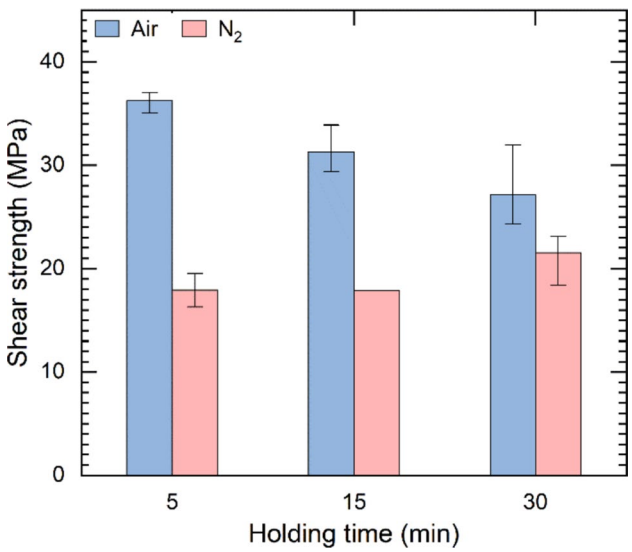

Figure 3 Shear strength of joints bonded in air and N_2 atmospheres, depending on the holding time during bonding.

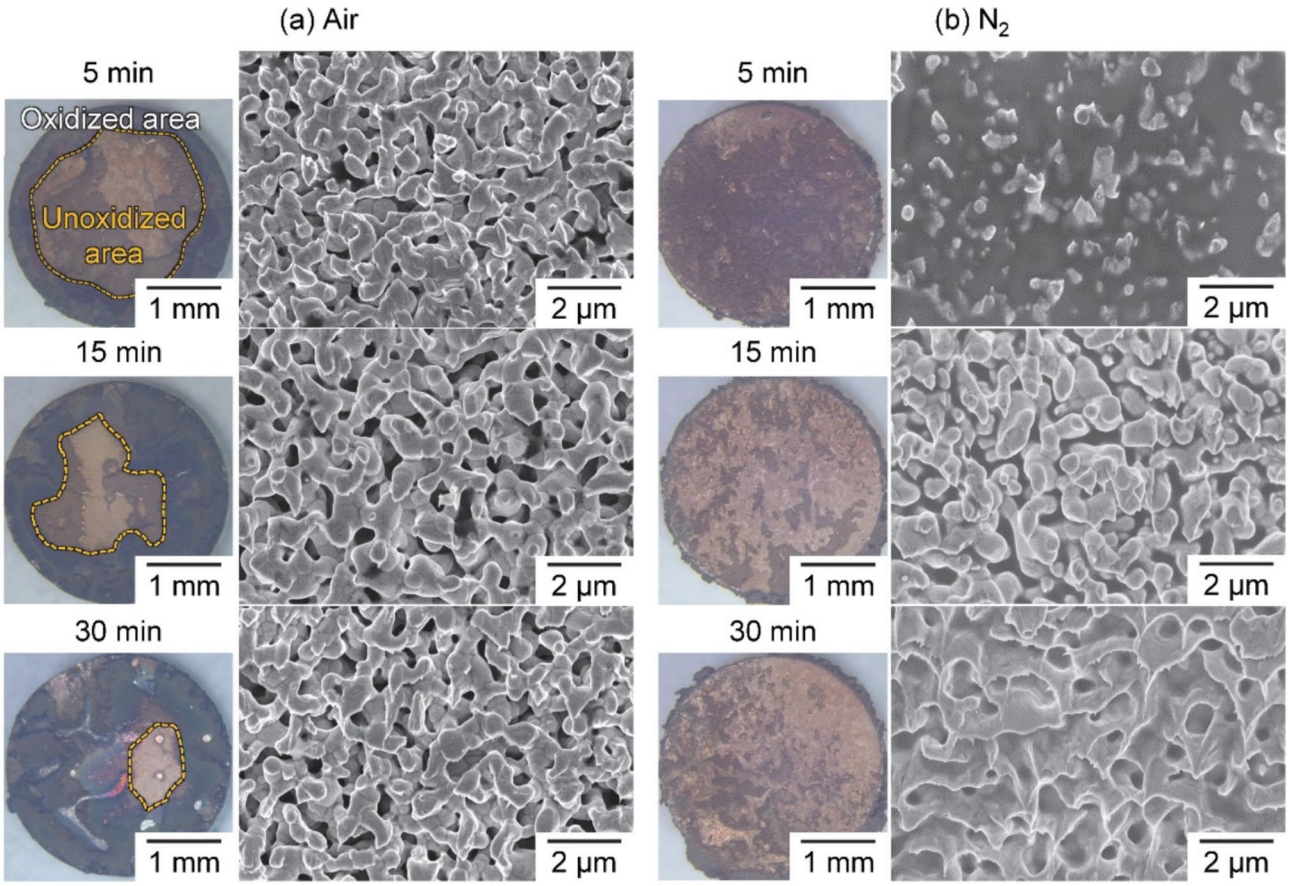

Figure 4 SM and SEM images of the fractured surface of joints bonded in **a** air and **b** N_2 atmospheres, depending on the holding time.

indicative of sintered copper fracture, while the joint edge showed a black region corresponding to a fractured copper oxide area. Furthermore, as the holding time increased, a reduction in the central-sintered copper region was observed. In contrast, for bonding in N_2 atmosphere, oxidation at the joint edges was not observed, even with an increase in holding time. SEM observations of the fractured sintered copper regions indicated that no significant changes in the sintered structure were observed for bonding in air. However, for bonding in N_2, necking of the sintered grains progressed with increasing holding time. Additionally, residual organic solvent was observed to cover the sintered structure, even after prolonged holding times.

Previous studies have reported that oxidation during Cu sintering can be suppressed under pressurized conditions of 5 MPa [23]. However, as shown in this study, under low-pressure conditions where densification is difficult to achieve, suppressing the ingress of air is insufficient. Consequently, oxidation is thought to have progressively advanced into the joint interior with increasing holding time, for bonding in the air atmosphere.

In contrast, for bonding in the N_2 atmosphere, although high joint strength was not achieved due to the low availability of oxygen, oxidation did not progress. This lack of oxygen also prevented the combustion of the organic solvent, leading to its residual presence on the sintered structure.

Figure 5 shows the cross-sectional SEM images of sintered joints bonded in air and N_2 atmosphere by varying the holding time. As for the bonding in air, the thickness of the sintered layer increased with increasing holding time (Fig. 5a). The increase in sintered layer thickness is attributed to the volume expansion associated with the oxidation from Cu to Cu_2O [12]. Nanoparticles of several tens of nanometers were observed on the sintered surface after 5 and 15 min, but not after 30 min. These observations suggest that the nanoparticles observed during shorter holding times were Cu_2O formed via oxidation during bonding, and that these Cu_2O nanoparticles grew to form

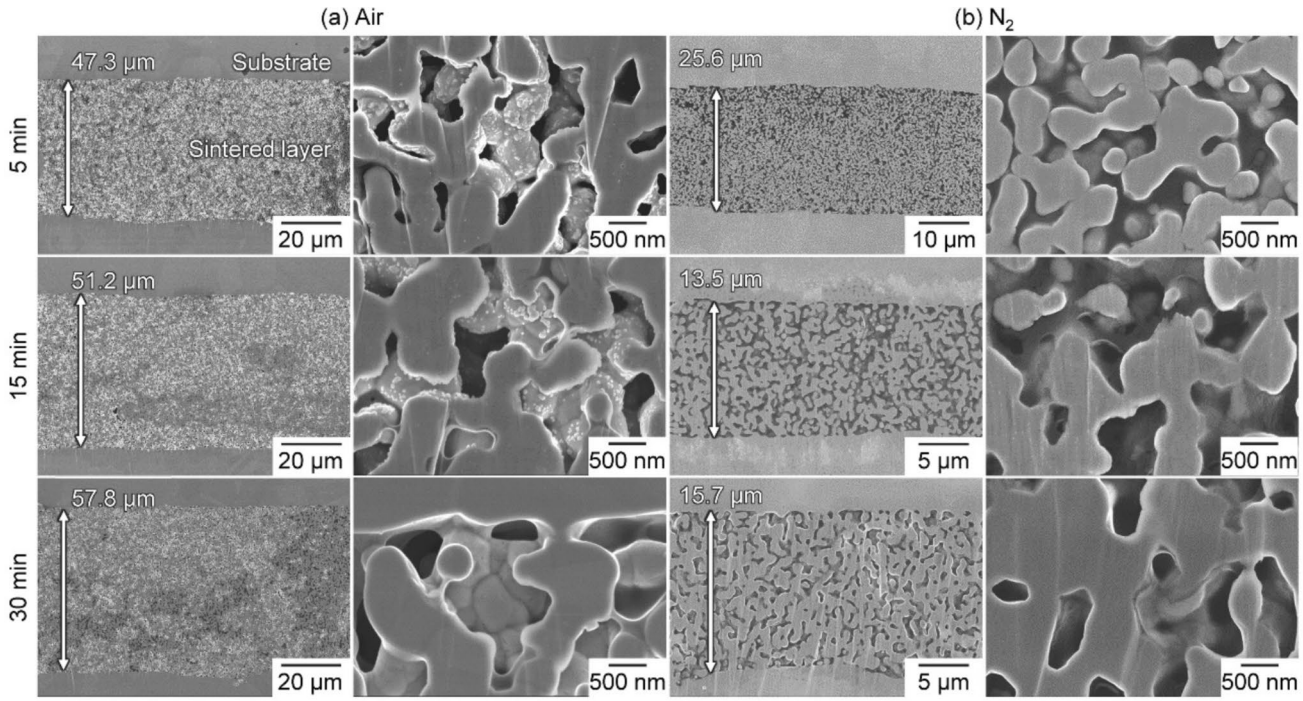

Figure 5 Cross-sectional SEM images of the joints bonded in **a** air and **b** N_2 atmospheres, depending on the holding time during bonding.

a continuous Cu_2O film on the surface of the sintered layer. Thus, it is hypothesized that the oxidation of Cu proceeded progressively from the surface of the sintered layer in the low-pressure bonding process in air.

At a holding time of 5 min, the joints bonded under a nitrogen atmosphere exhibited a porous sintered structure, indicating insufficient bonding between Cu particles and with the substrate. As the holding time increased to 15 min, the sintered layer became thinner and more compact. With further increases in holding time, the thickness remained nearly constant, while the microstructure continued to densify. The initial reduction in layer thickness is attributed to the evaporation of residual organic solvent, which is less prone to combustion under nitrogen, and the subsequent shrinkage due to sintering between particles. As sintering progressed, the rate of shrinkage decreased, leading primarily to an increase in density rather than a further reduction in thickness.

It is noted that the joints bonded under N_2 atmosphere still contained the organic solvent even at the holding time of 30 min compared to joints bonded in air. To evaluate the remaining organic solvents after bonding, TG–DTA analyses were performed on the bonding paste heated under air and N_2 atmospheres (Fig. 6). Under an ambient atmosphere, a

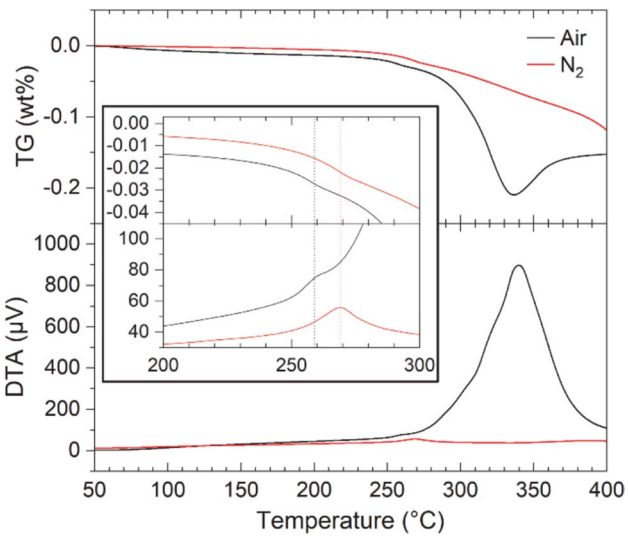

Figure 6 TG–DTA curves for bonding paste measured in **a** air and **b** N_2 atmospheres.

minor exothermic reaction accompanied by a slight weight loss was observed around 260 °C, followed by a prominent exothermic peak near 340 °C. After this point, the sample exhibited a weight increase. This indicates that complete combustion of the organic solvent occurs around 340 °C, leading to

the re-oxidation of Cu. In contrast, under a nitrogen atmosphere, an exothermic peak was observed around 270 °C, while no significant high-temperature exothermic reaction was detected. Therefore, the reaction occurring at 260–270 °C is attributed to a redox reaction between the organic solvent and the surface oxide layer. The high-temperature reaction observed only in air corresponds to the complete combustion of the organic solvent and the subsequent reoxidation of Cu induced by atmospheric oxygen.

These thermogravimetric and calorimetric analyses suggest that, under nitrogen, the combustion of the organic solvent is substantially suppressed, resulting in the retention of residual solvent within the bonded structure after the sintering process. This residual solvent is expected to delay the oxidation of the sintered Cu structure during subsequent thermal aging in air.

Characteristic changes during high-temperature storage

For the evaluation of heat resistance, Fig. 7 shows the changes in the shear strength of joints and the porosity in the joints subjected to high-temperature storage tests after bonding in air or N_2 atmosphere. The porosity was determined from cross-sectional observations of the sintered layers, as described later. Similar to the effect of holding time during bonding shown in Fig. 3, the joint strength decreased as the storage time increased for bonding in air. In contrast, for bonding in N_2, the joint strength increased with longer storage

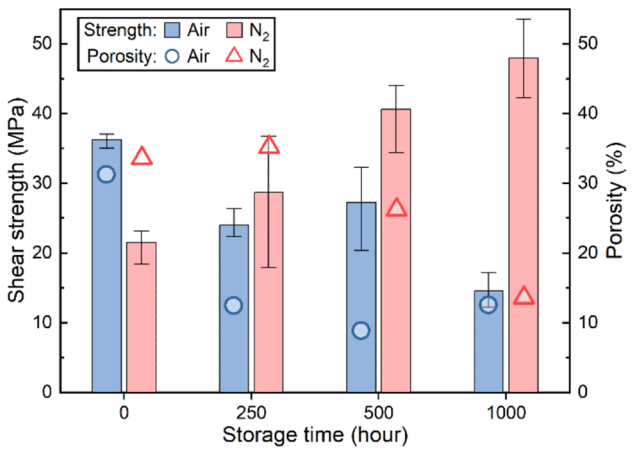

Figure 7 Changes in the shear strength of joints and the porosity of the sintered layer after high-temperature storage.

times. Porosity in the air-bonded joints decreased immediately after high-temperature storage, whereas in the nitrogen-bonded joints, it was initially maintained but gradually decreased with increasing storage time. It is noteworthy that the trend in strength variation does not necessarily coincide with that of porosity change.

The relationship between changes in joint strength and oxidation behavior during the high-temperature storage test was investigated through fractographic observations and XRD analyses of the fractured surfaces. In the XRD analysis, oxidation progression was quantified using the intensity ratio of $Cu_2O(111)$ to Cu(111) in the XRD profile as an indicator.

Figure 8 presents the analytical results of the fracture surfaces following the shear test. Figure 8a and b present the XRD profiles obtained from the fracture surfaces after high-temperature storage tests and the corresponding oxidation progression over time, respectively. Initially, the joints exhibited negligible Cu_2O peaks revealing low oxidation progression, whereas oxidation progressed upon high-temperature storage. The extent of this increase was dependent on the bonding atmosphere: in air, a substantial rise in the Cu_2O peak intensity was observed, whereas in N_2, the increase in Cu_2O intensity remained marginal. Figure 8c and d presents the stereomicroscopic and SEM observations of the fracture surfaces after 1000 h of storage. The fracture surfaces of air-bonded joints exhibited a distinct black coloration, and detailed SEM observations revealed the presence of fine nano-oxide layers covering the Cu substrate. In contrast, the fracture surfaces of N_2-bonded joints showed traces of ductile fracture, such as elongated sintered Cu grains, even after 1000 h of storage.

Based on the oxidation progression and fractographic analyses, it can be concluded that, for air-bonded joints, oxidation progressed significantly with increasing high-temperature storage time, resulting in the formation of brittle regions. On the contrary, in N_2-bonded joints, although oxidation occurs to some extent, excessive oxidation is effectively suppressed. Furthermore, grain boundary sintering progresses within the sintered layer, thereby contributing to improved joint strength.

Figure 9 presents the microstructural evolution of the sintered Cu layer during the high-temperature storage in ambient air and N_2 atmospheres. Significant densification of the sintered layer was observed in both conditions; however, distinct differences in

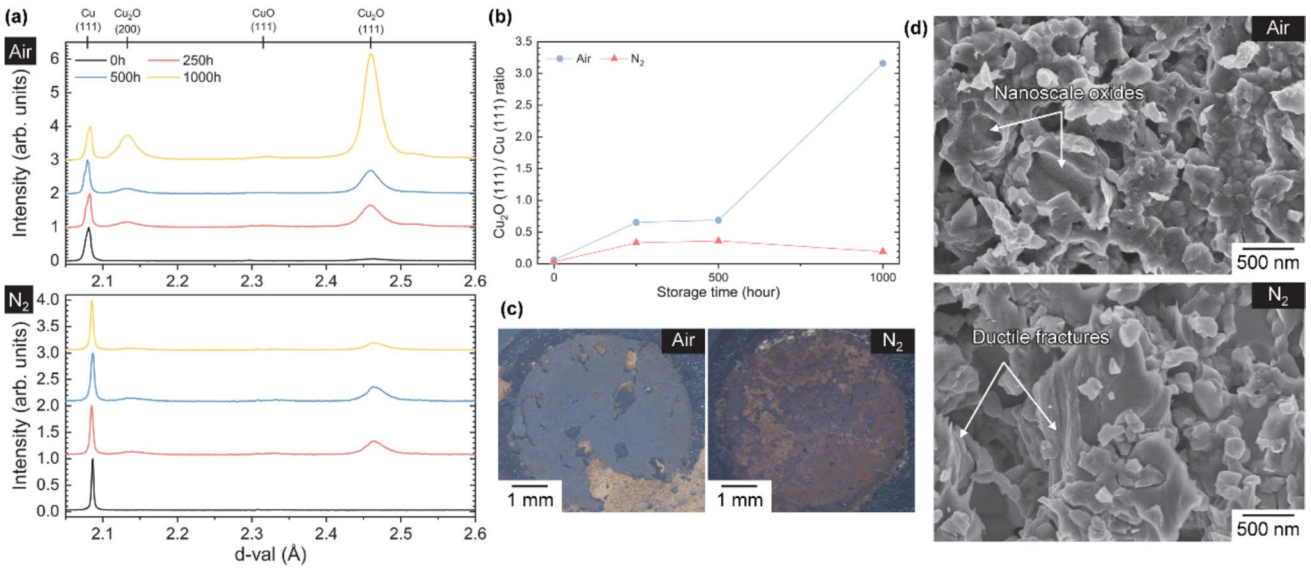

Figure 8 Oxidation behavior of joints bonded in air and N_2 atmospheres after high-temperature storage. **a** XRD patterns of the fractured surfaces. **b** Intensity ratio of Cu_2O (111) to Cu (111). Representative fractured surfaces after 1000 h of storage observed by **c** SM and (d) SEM

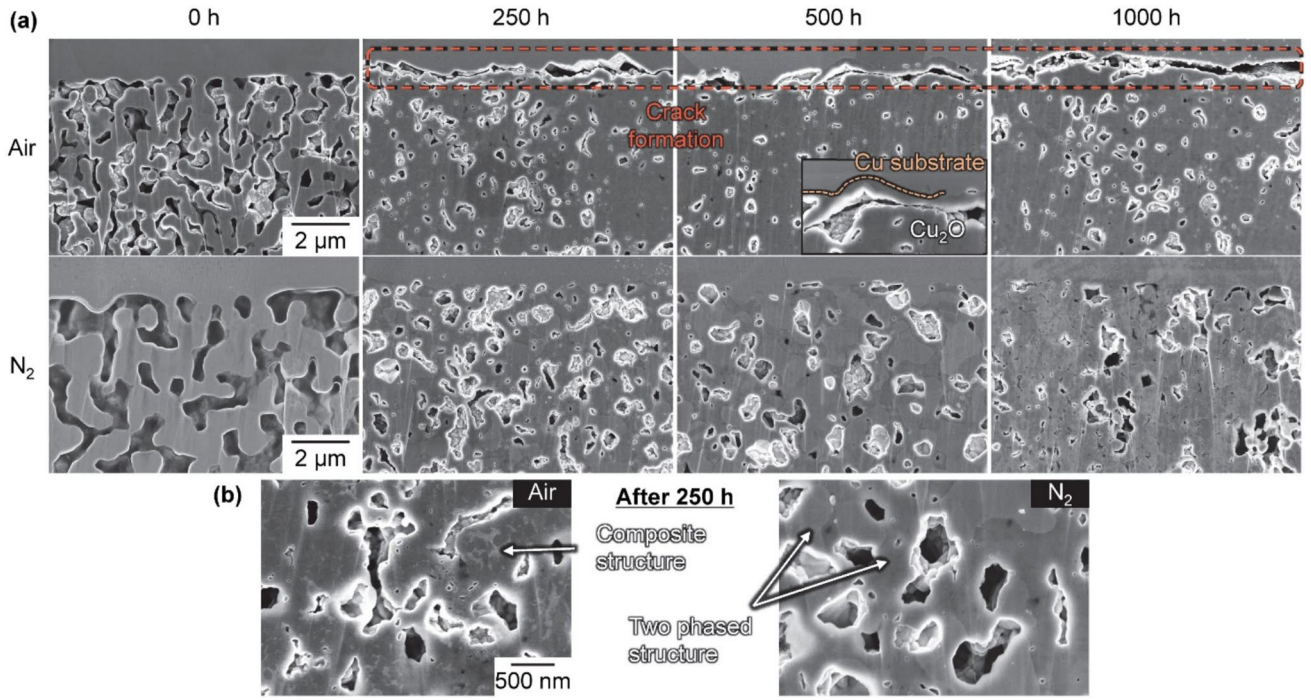

Figure 9 Microstructural evolution of the sintered Cu layer during the high-temperature storage in ambient air and N_2 atmospheres. **a** Overview of microstructural evolution. **b** Difference in the sintered structure after 250 h of storage.

oxidation behavior and crack formation were identified (Fig. 9a). In air-bonded joints, coarse cracks were observed at the interface. Enlarged images after 500 h of storage revealed the formation of an oxide layer at the interface. In contrast, no significant crack formation was observed at the interface of joints bonded in N_2, indicating that sufficient interfacial bonding was maintained. Figure 9b compares the sintered

microstructure within the sintered layer after 250 h of storage, highlighting the differences in the structure between bonding in air and in N_2 atmosphere.

For air-bonded joints, the structure exhibited a mixture of regions with different contrasts. In particular, dark regions near voids appeared to penetrate and erode the bright regions within the sintered grains. Based on XRD analysis and fractographic observations after high-temperature storage, it is considered that densification in air-bonded joints was primarily caused by oxidation. According to previous research [25], the oxidation of Cu joints progresses from voids during high-temperature storage. The brittle Cu oxide that forms exhibits a larger molar volume than the sintered Cu formed during bonding, resulting in compressive stress within the oxide layer during storage. Upon cooling to room temperature, the difference in the coefficient of thermal expansion (CTE) between Cu and Cu_2O, where Cu exhibits greater shrinkage, causes thermal compressive stress within the oxide layer. Consequently, stress induced by the differences in molar volume and CTE between Cu oxides and sintered Cu is suggested to cause crack formation. Similarly, in the air-bonded joints of this study, oxidation progressed from voids at the interface, and cracks are considered to have developed during the cooling process due to the stress generated by differences in molar volume and CTE between Cu and Cu_2O.

In contrast, for joints bonded in N_2 atmosphere, the structure did not appear to be a fully mixed phase as observed in air-bonded joints. Instead, a distinct two-phase structure with different contrasts was identified. After 1000 h of storage, some expansion of the dark regions and the formation of small voids within the sintered phase were observed. This suggests that the bright regions correspond to the original Cu-sintered phase, while the dark regions are associated with oxidation-induced phases. However, unlike air-bonded joints, the two phases did not progress toward a fully mixed and single-phase structure. In other words, although oxidation progressed from initial void regions in the sintered layer, the progression rate was significantly lower than that observed in air-bonded joints, and interfacial oxidation severe enough to induce crack formation was effectively suppressed.

Figures 10 and 11 present TEM images of Cu-sintered joints bonded in air and N_2 after thermal storage for 500 h. Figures 10b and 11b display high-resolution TEM images for both joints obtained from Region A in Figs. 10a and 11a. Fast Fourier Transform (FFT) images of Regions C (sintered layer) and D (substrate) show the formation of Cu_2O in the vicinity of the interface even for the joint bonded in N_2. The oxidation results were confirmed by EDX elemental maps, analyzing region B, as shown in Figs. 10c and 11c. However, oxidation behavior in joints bonded in N_2 differed from that in air. Figures 10d and 11d present STEM images of sintered joints and nanobeam diffraction (NBD) patterns obtained at Points E and F. While the joint bonded in air exhibited that the sintered layer was thoroughly oxidized to Cu_2O, the joint bonded in N_2 comprised both Cu and Cu_2O nanocrystalline grains, revealing the suppression of oxidation, which was consistent with SEM observation results.

Figure 12 shows the change in volume resistivity with increasing thermal storage time. As expected from the observation results, the resistivity of joints bonded in air increased tenfold after storage compared with that before the storage. In contrast, the resistivity of joints bonded in N_2 was maintained even after storage and was rather improved compared with the initial value.

As shown in Fig. 7, porosity decreased with increasing storage time. In general, a decrease in porosity is generally accompanied by a reduction in electrical resistivity. However, based on the microstructural and XRD analyses, the porosity reduction observed in Fig. 7 is attributed to the volume expansion associated with Cu oxidation, during which Cu is replaced by Cu_2O, which possesses inherently higher resistivity. Under these conditions, the influence of porosity reduction on maintaining electrical conductivity is expected to be insignificant, as confirmed by the increase in resistivity observed in the air-bonded joints. Accordingly, we successfully suppressed the degradation of the electrical properties of low-pressure Cu sinter joints during high-temperature storage in air by utilizing the Cu sinter bonding process under N_2 atmosphere with the use of PEG400.

We discuss the possible mechanism governing the development of oxidation resistance in the present Cu sinter bonding process as shown in Fig. 13. For joints fabricated under ambient air conditions, partial coverage of the sintered Cu particle surfaces by an organic residue film occurs due to interfacial reactions between the oxidized Cu and PEG400. However, under prolonged thermal exposure, direct contact of the exposed Cu surfaces with atmospheric oxygen is expected to accelerate oxidation. The growth of oxide regions over time induces stress accumulation at the

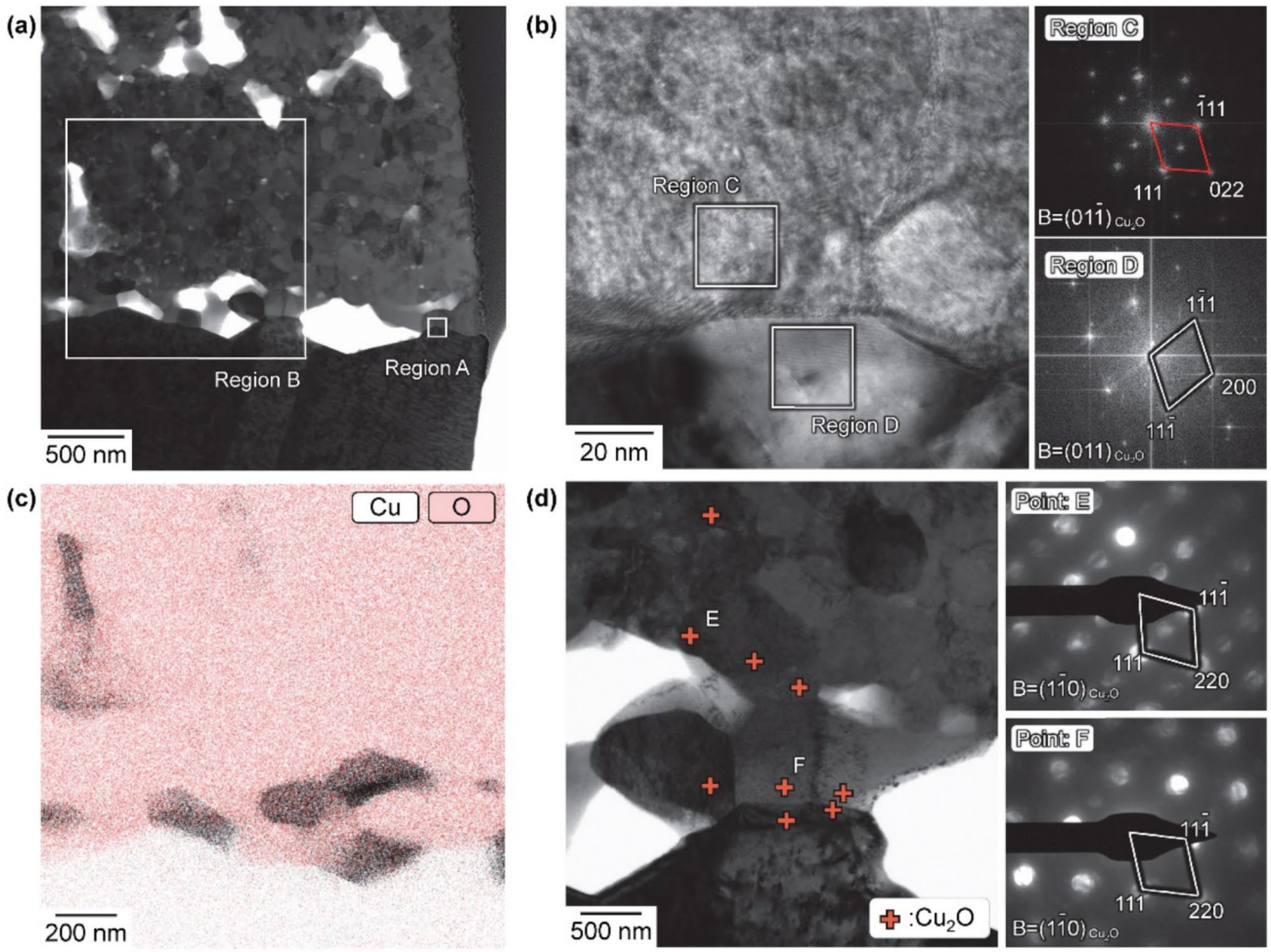

Figure 10 TEM analyses of Cu sintered joints bonded in air after thermal storage for 500 h. **a** BF-STEM overview image of the sintered layer. **b** HR-TEM image of the interface and corresponding FFT patterns obtained from Regions C and D. **c** EDX elemental maps of Cu and O for the joint. **d** BF-STEM image highlighting structures identified by nanobeam diffraction at Points E and F.

Cu/Cu_2O interfaces, primarily due to mismatches in molar volume and coefficients of thermal expansion [25]. These interfacial stresses are likely to promote crack initiation and propagation within the joint. Consequently, both mechanical properties and electrical conductivity deteriorate as degradation progresses.

In contrast, in the joints bonded under a nitrogen atmosphere, the reductive bonding environment enables residual PEG400 to remain in the vicinity of the sintered microstructure. Organic protective layers formed on the surface of Cu particles have been proposed as an effective strategy for suppressing oxidation during Cu sinter bonding. In particular, the formation of such layers on the sintered Cu structure—either through particle surface treatment or paste modification using reducing solvents—has been actively investigated [5, 6, 9, 24]. Wang et al. employed lactic acid to impart both reductive functionality and oxidation resistance to Cu nanoparticle joints. Lactic acid effectively removed surface oxides from the synthesized Cu nanoparticles and formed copper lactate, which inhibited oxidation during the heating and holding stages of the bonding process. At elevated temperatures, the copper lactate subsequently decomposed into metallic Cu, resulting in a purified Cu structure [9].

During subsequent thermal aging in ambient air, this residual reductant reacts with incoming oxygen and/or surface oxides, which in turn delays the progression of oxidation compared to the air-bonded

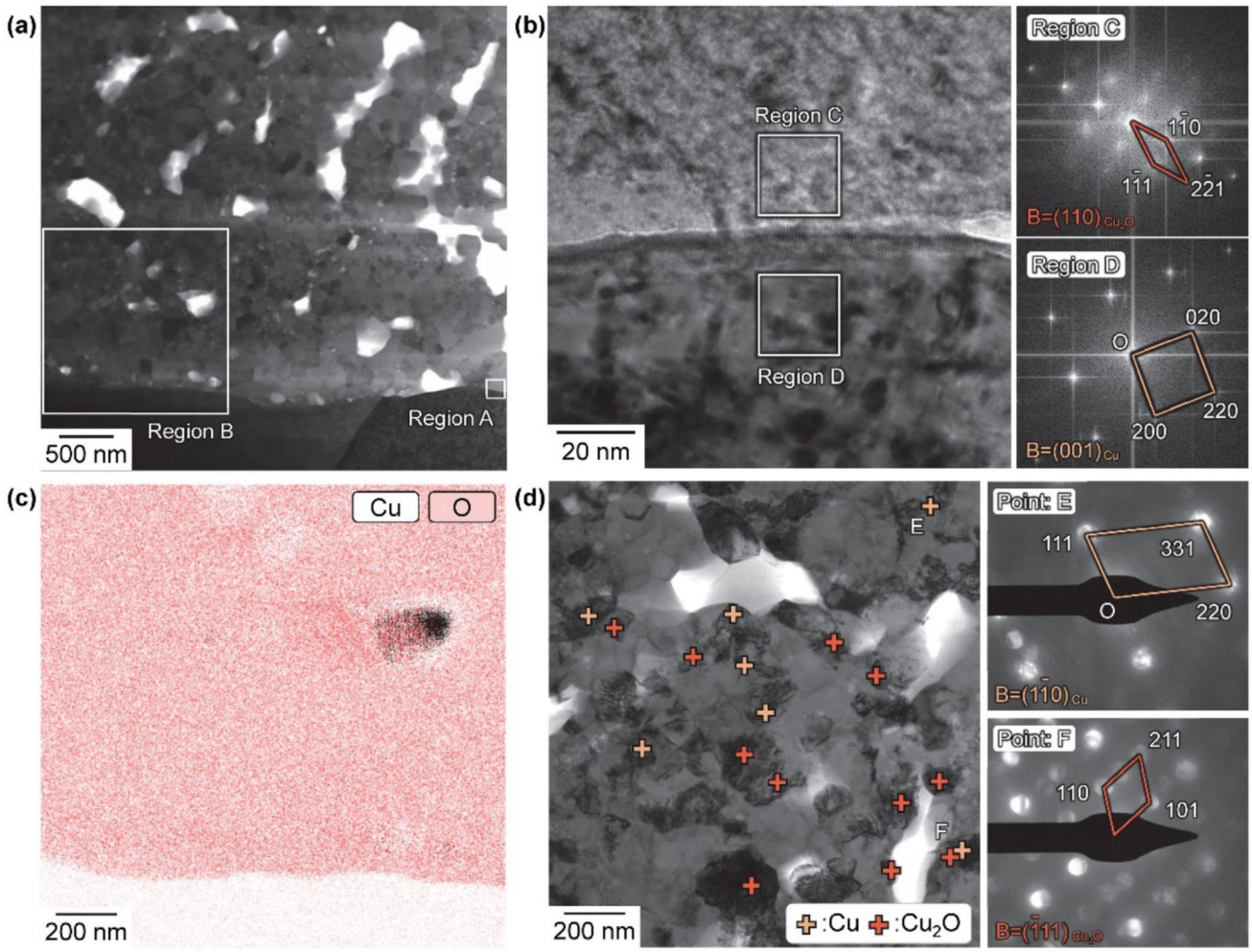

Figure 11 TEM analyses of Cu-sintered joints bonded in N_2 after thermal storage for 500 h. **a** BF-STEM overview image of the sintered layer. **b** HR-TEM image of the interface and corresponding FFT patterns obtained from Regions C and D. **c** EDX elemental maps of Cu and O for the joint. **d** BF-STEM image highlighting structures identified by nanobeam diffraction at Points E and F.

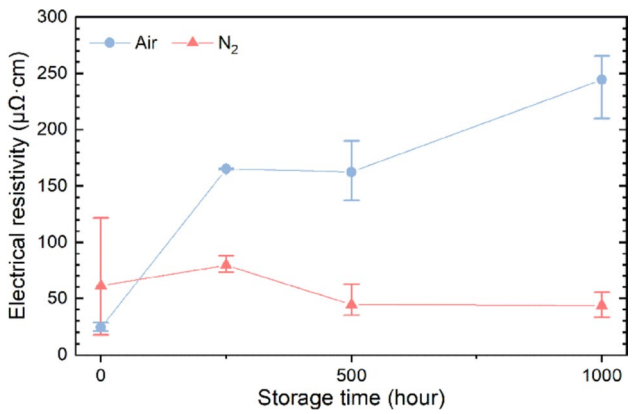

Figure 12 Electrical resistivity of joints after high-temperature storage.

joints. As a result, oxidation remains localized rather than widespread, and the sintered structure retains a composite morphology comprising metallic Cu and Cu_2O. Within this structure, the remaining metallic Cu forms a continuous skeletal network that ultimately governs both mechanical load transfer and electrical conduction, defining the overall performance of the joint.

Accordingly, this study demonstrated that the retention of residual reductants enhances the post-bonding oxidation resistance of low-pressure Cu sintered joints. However, joints bonded in nitrogen exhibited relatively low initial strength, highlighting the need for further densification of the sintered layer. As discussed above, this can be achieved by

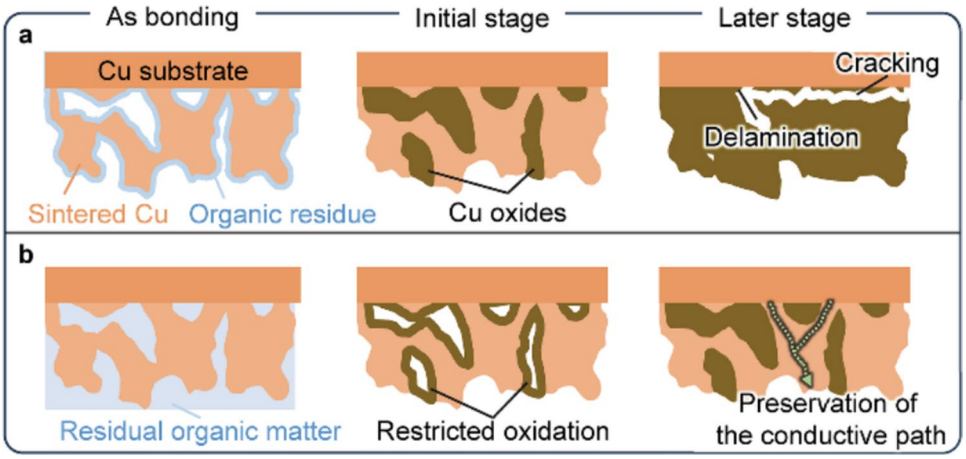

Figure 13 Schematic of microstructural changes during high-temperature storage of joints bonded in **a** air and **b** N_2 atmospheres.

prolonging the holding time during bonding to promote sintering without oxidation. For shorter bonding durations, on the other hand, particle-packing strategies that secure a sufficient fraction of organic solvents capable of resisting oxygen ingress during high-temperature exposure are considered effective. In terms of long-term stability, not only PEG400 itself but also its reaction residues, as reported in previous studies, are considered to contribute effectively to oxidation resistance. Nevertheless, the organic solvent employed in this study may not necessarily be the most effective option. Further exploration of oxidation-inhibiting organic solvents will be important for achieving even greater improvements in oxidation resistance.

Taking these approaches into account, the improved oxidation resistance identified in this work is expected to not only ensure high-temperature durability but also enhance the thermal reliability and fatigue life of electronic packages, including power devices and integrated modules, thereby facilitating the industrial implementation of Cu sinter bonding in applications demanding high reliability.

Conclusions

With increasing bonding time, joints bonded in nitrogen retained residual organic solvents in the sintered layer, enabling continued sintering, whereas those bonded in air experienced structural degradation due to oxidation.

TG–DTA analyses demonstrated that oxidation suppression in nitrogen-bonded joints was primarily attributed to the inhibited combustion of reducing solvents.

Under ambient air bonding conditions, rapid oxidation occurred within the sintered Cu joints during high-temperature exposure at 250 °C. This oxidation led to the formation of brittle Cu_2O layers, which significantly reduced both the mechanical integrity and electrical conductivity of the joints.

Bonding in a nitrogen atmosphere effectively suppressed oxidation due to the presence of residual reducing solvents. The retained organic solvents effectively delayed oxidation progression, thereby preserving mechanical strength and electrical conductivity even after prolonged thermal storage in air.

Microstructural analyses revealed the formation of a composite microstructure consisting of metallic Cu and localized Cu_2O phases under nitrogen bonding conditions. The metallic Cu phase remained structurally continuous, providing the mechanical load-bearing capacity and electrical conduction pathway, thus maintaining the joint's overall performance.

Data and code availability

The datasets generated and analyzed during the current study are available from the corresponding author upon reasonable request.

Acknowledgements

This work was supported in part by the Japan Society for the Promotion of Science (JSPS) KAKENHI (Grant Numbers 23K23100 and 25K01546) and Iketani Science

and Technology Foundation (Grant Number 0361033-A). This study was performed in part under the Cooperative Research Program of Institute for Joining and Welding Research Institute, Osaka University.

Author contributions

Conceptualization and funding acquisition were contributed by Tomoki Matsuda; Methodology, formal analysis, investigation, and writing – original draft preparation were involved by Tomoki Matsuda and Shio Okubo; writing—review and editing and supervision were performed by Makoto Kambara and Akio Hirose.

Funding

Open Access funding provided by The University of Osaka. Japan Society for the Promotion of Science,23K23100,Tomoki Matsuda,25K01546,Tomoki Matsuda, Iketani Science and Technology Foundation,0361033-A,Tomoki Matsuda

Declarations

Conflict of interest The authors declare that they have no known competing financial interests or personal relationships that could have appeared to influence the work reported in this paper.

References

[1] Allen GL, Bayles RA, Gile WW, Jesser WA (1986) Small particle melting of pure metals. Thin Solid Films 144:297–308. https://doi.org/10.1016/0040-6090(86)90422-0

[2] Lai SL, Guo JY, Petrova V, et al (1996) Size-Dependent Melting Properties of Small Tin Particles : Nanocalorimetric Measurements. 99–102

[3] Chen TF, Siow KS (2021) Comparing the mechanical and thermal-electrical properties of sintered copper (Cu) and sintered silver (Ag) joints. J Alloys Compd 866:158783. https://doi.org/10.1016/j.jallcom.2021.158783

[4] Gao Y, Li W, Chen C et al (2018) Novel copper particle paste with self-reduction and self-protection characteristics for die attachment of power semiconductor under a nitrogen atmosphere. Mater Des 160:1265–1272. https://doi.org/10.1016/j.matdes.2018.11.003

[5] Mou Y, Liu J, Cheng H et al (2019) Facile preparation of self-reducible Cu nanoparticle paste for low temperature Cu-Cu bonding. JOM 71:3076–3083. https://doi.org/10.1007/s11837-019-03517-5

[6] Li J, Liang Q, Shi T et al (2019) Design of Cu nanoaggregates composed of ultra-small Cu nanoparticles for Cu-Cu thermocompression bonding. J Alloys Compd 772:793–800. https://doi.org/10.1016/j.jallcom.2018.09.115

[7] Li J, Yu X, Shi T et al (2017) Low-temperature and low-pressure Cu–Cu bonding by highly sinterable Cu nanoparticle paste. Nanoscale Res Lett 12:0–5. https://doi.org/10.1186/s11671-017-2037-5

[8] Liu X, Nishikawa H (2017) Pressureless sintering bonding using hybrid microscale Cu particle paste on ENIG, pure Cu and pre-oxidized Cu substrate by an oxidation–reduction process. J Mater Sci Mater Electron 28:5554–5561. https://doi.org/10.1007/s10854-016-6220-8

[9] Wang X, Zhang Z, Feng Y, Xiao F (2022) Anti-oxidative copper nanoparticle paste for Cu–Cu bonding at low temperature in air. J Mater Sci Mater Electron 33:817–827. https://doi.org/10.1007/s10854-021-07352-w

[10] Gao Y, Takata S, Chen C et al (2019) Reliability analysis of sintered Cu joints for SiC power devices under thermal shock condition. Microelectron Reliab 100:113456. https://doi.org/10.1016/j.microrel.2019.113456

[11] Choudhary S, Sarma JVN, Pande S et al (2018) Oxidation mechanism of thin Cu films: a gateway towards the formation of single oxide phase. AIP Adv. https://doi.org/10.1063/1.5028407

[12] Unutulmazsoy Y, Cancellieri C, Lin L, Jeurgens LPH (2022) Reduction of thermally grown single-phase CuO and Cu_2O thin films by in-situ time-resolved XRD. Appl

Surf Sci 588:152896. https://doi.org/10.1016/j.apsusc.2022.152896

[13] Li W, Li L, Gao Y et al (2018) Highly conductive copper films based on submicron copper particles/copper complex inks for printed electronics: microstructure, resistivity, oxidation resistance, and long-term stability. J Alloys Compd 732:240–247. https://doi.org/10.1016/j.jallcom.2017.10.193

[14] Gao Y, Jiu J, Chen C et al (2022) Oxidation-enhanced bonding strength of Cu sinter joints during thermal storage test. J Mater Sci Technol 115:251–255. https://doi.org/10.1016/j.jmst.2021.10.047

[15] Gao R, He S, Li J et al (2020) Interfacial transformation of preoxidized Cu microparticles in a formic-acid atmosphere for pressureless Cu–Cu bonding. J Mater Sci Mater Electron 31:14635–14644. https://doi.org/10.1007/s10854-020-04026-x

[16] Xie J, Shen J, Deng J, Chen X (2020) Influence of aging atmosphere on the thermal stability of low-temperature rapidly sintered Cu nanoparticle paste joint. J Electron Mater 49:2669–2676. https://doi.org/10.1007/s11664-020-07951-z

[17] Yao T, Matsuda T, Sano T et al (2018) In situ study of reduction process of CuO paste and its effect on bondability of Cu-to-Cu joints. J Electron Mater. https://doi.org/10.1007/s11664-017-6049-9

[18] Liu X, Nishikawa H (2016) Low-pressure Cu-Cu bonding using in-situ surface-modified microscale Cu particles for power device packaging. Scr Mater 120:80–84. https://doi.org/10.1016/j.scriptamat.2016.04.018

[19] Yonezawa T, Tsukamoto H, Matsubara M (2015) Low-temperature nanoredox two-step sintering of gelatin nanoskin-stabilized submicrometer-sized copper fine particles for preparing highly conductive layers. RSC Adv 5:61290–61297. https://doi.org/10.1039/c5ra06599b

[20] Fujimoto T, Ogura T, Sano T et al (2015) Joining of pure copper using Cu nanoparticles derived from CuO paste. Mater Trans 56:992–996. https://doi.org/10.2320/matertrans.MI201410

[21] Yamagiwa D, Matsuda T, Furusawa H et al (2021) Pressureless sinter joining of bare Cu substrates under forming gas atmosphere by surface-oxidized submicron Cu particles. J Mater Sci Mater Electron 32:19031–19041. https://doi.org/10.1007/s10854-021-06418-z

[22] Matsuda T, Yamagiwa D, Furusawa H et al (2022) Reduction behavior of surface oxide on submicron copper particles for pressureless sintering under reducing atmosphere. J Electron Mater. https://doi.org/10.1007/s11664-021-09274-z

[23] Matsuda T, Yamada S, Okubo S, Hirose A (2023) Antioxidative copper sinter bonding under thermal aging utilizing reduction of cuprous oxide nanoparticles by polyethylene glycol. J Mater Sci 58:15617–15633. https://doi.org/10.1007/s10853-023-08976-5

[24] Liu J, Chen H, Ji H, Li M (2016) Highly conductive Cu-Cu joint formation by low-temperature sintering of formic acid-treated Cu nanoparticles. ACS Appl Mater Interfaces 8:33289–33298. https://doi.org/10.1021/acsami.6b10280

[25] Liu X, Zhou S, Nishikawa H (2017) Thermal stability of low-temperature sintered joint using Sn-coated Cu particles during isothermal aging at 250 °C. J Mater Sci Mater Electron 28:12606–12616. https://doi.org/10.1007/s10854-017-7085-1